AIAA 2001–0510

AN OVERVIEW OF COMPUTATIONAL AEROACOUSTIC TECHNIQUES APPLIED TO CAVITY NOISE PREDICTION

Sheryl M. Grace
Aerospace and Mechanical Engineering Department
Boston University, 110 Cummington St., Boston, MA 02215

39th AIAA Aerospace Sciences Meeting and Exhibit
January 8-11, 2001/Reno, NV

AN OVERVIEW OF COMPUTATIONAL AEROACOUSTIC TECHNIQUES APPLIED TO CAVITY NOISE PREDICTION

Sheryl M. Grace*
Aerospace and Mechanical Engineering Department
Boston University, 110 Cummington St., Boston, MA 02215

This report contains a summary of recent advances in the development of computational aeroacoustic methods for predicting the vibration and acoustics associated with grazing flow past cavities. The applications for which this flow field applies vary greatly and thus many Mach number regimes and cavity geometries are discussed. In addition to the computational developments, recent experimental studies are discussed. The results of many of these experiments can be used for validation of present and future prediction tools.

Introduction

GRAZING flow past a cavity may create both broadband and tonal noise. The formation and behavior of a shear layer and its subsequent interaction with the fluid in the cavity and the solid walls bounding the cavity drives the noise production. Thus cavity noise prediction algorithms must resolve the shear-layer behavior well. As such, the prediction of this noise becomes more feasible with continued advanced in computational capabilities.

Many computational studies focus on the computation of the cavity flow field with little attention given to the acoustic field surrounding the cavity. Exceptions do exist, including several studies aimed at computing the acoustics from low and subsonic Mach number flows past cavities[1–4] and another method valid for all subsonic Mach numbers.[5] While there are seemingly few articles focusing on acoustic field predictions, numerous articles have been written on the computational of cavity flows. The cavity flow simulations that focus on the *near field* are equally important to the development of a noise prediction capability for cavity flows; for, if the near-field flow is not simulated properly, one cannot hope to predict the acoustic field accurately. In this sense, advances in computational fluid dynamic (CFD) modeling go hand-in-hand with advancing computational aeroacoustic (CAA) methods. Therefore this review encompasses both CFD and CAA treatments of cavity flows.

The development of computational models also requires experimental data. Again, experimental cavity flow research is dominated by the study of near-field flow oscillations and cavity-wall pressure fluctuations. A notable exception is the research reported in [Ref.6]. With the intent of providing the reader with a list of possible sources for obtaining benchmarking data, section 3 of this article is devoted to describing some of these experiments. Because prior reviews by Heller and Bliss,[7] Rockwell and Naudascher[8] and Komerath et al.[9] contain an extensive review of experimental findings prior to 1987, this review focuses on experiments reported since 1987.

This paper contains three main sections. The first gives a general overview of the characterization of cavity flows. The second, reviews recent experiments. And the third section reviews the recent computational research.

Characterization of cavity flow

THE great interest in cavity flows and the large number of papers devoted to this subject stem from the wide number of applications subject to this type of flowfield. These include, but are not limited to, automobile components, gas transport systems, aircraft wheel and weapon bays, and aircraft research telescope/radar cavities. In all of these applications, the designer would like to eliminate the occurrence of high pressure amplitude oscillations because they lead to unsteady loadings on components within or near the cavity or because they lead to unwanted sound.

The flow field due to grazing flow past a cavity has been characterized previously. Rockwell and Naudascher[8] identified three flow regimes which they labeled fluid-dynamic interactions, fluid-resonant iterations, and fluid-elastic interactions. The fluid-dynamic regime involves shear-layer instability amplification due to feedback from interaction of the shear layer with the aft cavity wall. Such interaction often occurs for low-speed flow past shallow cavities. The fluid-resonant regime couples the acoustic modes of the cavity and the shear layer over the cavity. This interaction occurs for deeper cavities and for cavities subject to high Mach number grazing flow. The fluid-elastic regime encompasses flows that are affected by the elastic boundaries of the cavity. This phenomenon is most often encountered when one part of the cavity is being actuated like the based of the cavity being forced as a piston.

The parameters that are used to define the *shallow*

*Assistant Professor, Member AIAA.

and *deep* cavity regimes and their cut-off values are up for debate. According to Sarohia[10] shallow cavities have length-to-depth (L/D) ratios less than 1.0 while deep cavities have L/D ratios greater than 1.0. Rossiter,[11] on the other hand, defines the cutoff to be a ratio of 4.0.

The fluid-dynamic and fluid-resonant interaction regimes are encountered often in practice. The interactions present in these regimes can lead to large unsteady pressure forces and the production of high amplitude tones. Hence prediction and subsequent control of this type of cavity flow warrants attention. Past research has lead to the other classification of cavity flows as well. These classifications are identified based on the shear-layer's behavior.

At low speeds, the cavity has been classified as responding in either *shear-layer mode* or *wake mode*. For the shear-layer mode, the shear layer spans the mouth of the cavity and stagnates at the aft wall. In this classification, the shear-layer mode can encompass both the fluid-dynamic and fluid-resonant regimes. The wake mode is identified by the stagnation of the flow prior to the aft wall (i.e., reattachment of the shear layer to the cavity base). Researchers such as Gharib and Roshko[12] noted the flow looked similar to a bluff-body wake, hence the mode name. In the wake mode, self oscillations cease, the cavity flow "becomes unstable on a large scale", and the drag due to the presence of the cavity greatly increases.

For transonic and supersonic flows where shocks form above the cavity, cavity flows have been classified as open, closed, transitionally open, and transitionally closed.[13] Figures 1 and 2 show sketches reproduced from [Ref.13] depicting the different cavity flow types. Open cavities, like cavities operating in the shear-layer mode, are characterized by shear-layer reattachment at the downstream wall. At supersonic speed, a weak shock wave can form near the leading edge of the cavity. A nearly uniform static pressure distribution is produced which is desirable in practice; however, high intensity acoustic tones can develop.[13]

Closed cavities are characterized by reattachment of the shear layer on the cavity floor with a secondary separation prior to the downstream wall. At supersonic speeds, this creates an adverse static pressure gradient. For munitions deployed from shallow bays, this can cause large nose-up pitching moments. However, no acoustics tones are present for closed cavities.[13]

Transitionally closed cavity flow is characterized by the coalescence of the impingement shock and the exit shock into a single shock. Transitionally open cavity flow, on the other hand, contains a series of expansion and compression wavelets in place of the exit shock wave.[13]

Initially, the cut-off for these regimes were though to be given by specific values of the length-to-depth ra-

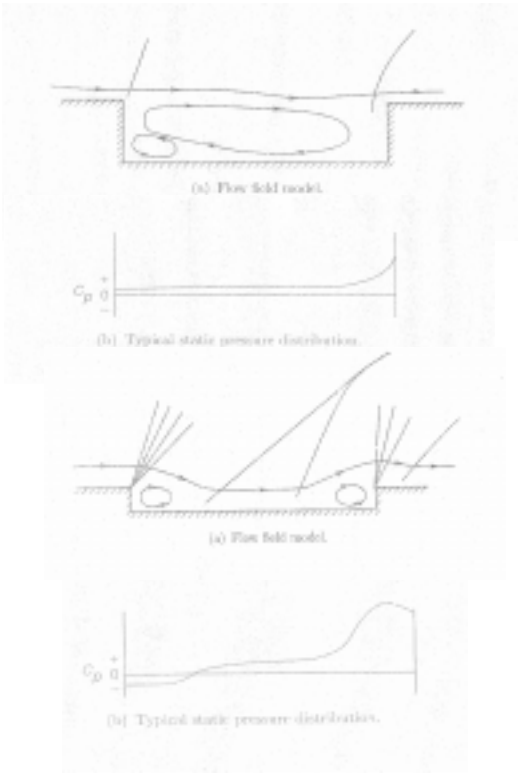

Fig. 1 Open (top) and closed (bottom) cavity flow field and nominal cavity floor pressure.

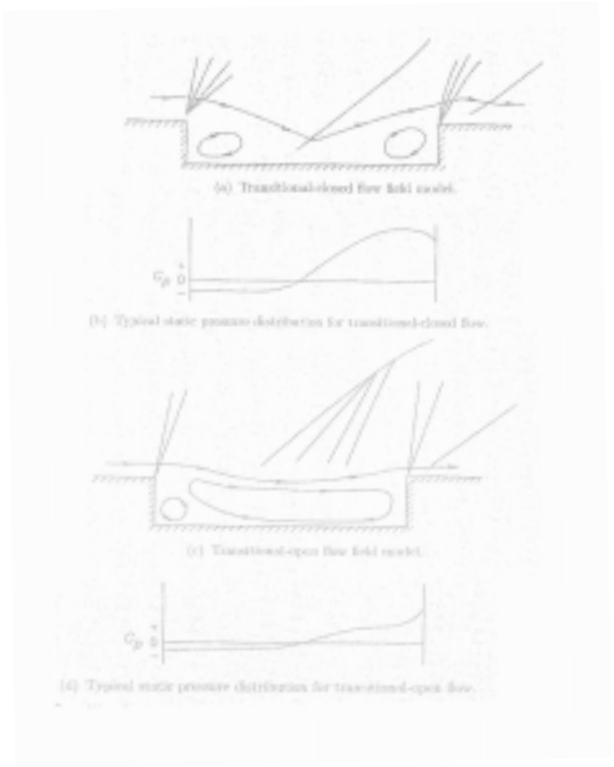

Fig. 2 Transitionally closed (top) and transitionally open (bottom) cavity flow field and nominal cavity floor pressure.

tio L/D. In the literature though, one can find vastly different values reported. For instance: $L/D < 10$ for open and $L/D > 13$ for closed,[13] $L/D < 9$ for open and $L/D > 13$ for closed,[14] $L/D < 3$ for open and $L/D > 10$ for closed.[15] Recently, Tracy and Plentovich[16] and Raman et al.[17] have concluded that the disagreement found in the literature stems from the dependence of the cavity flow type on Mach number as well as L/D.

For open cavities and cavities operating in the shear-layer mode, empirical formulae exist for predicting the frequency of oscillation. For deeper cavities, the natural frequency of the cavity, i.e., acoustic depth modes, are observed.[18] The frequency of these oscillations are governed by

$$f = \frac{c_0}{L}\frac{(2m-1)}{4}$$

where c_0 is the speed of sound, and m is the mode number. For cavities with larger length-to-depth ratios, in which the shear layer still spans the cavity opening, shear-layer modes dominate the spectrum. The frequencies of these modes for higher speed flows ($M < 0.4$) are well approximated by the Rossiter equation

$$f = \frac{U}{L}\frac{m-\alpha}{M+1/\kappa} \tag{0.1}$$

where U is the exterior flow speed, m is the mode number and Rossiter defined α and κ experimentally as 0.25 and 0.57 respectively. α accounts for the phase lag between the passage of a disturbance past the cavity trailing edge and the formation of its corresponding upstream traveling disturbance (in fractions of wavelengths). κ is the ratio of the disturbance convection speed to the freestream velocity. A modified version of Rossiter's equation,

$$f = \frac{U}{L}\frac{m-\alpha}{\frac{M}{\sqrt{1+\frac{\gamma-1}{2}M^2}}+\frac{1}{\kappa}} \tag{0.2}$$

with γ representing the ratio of specific heats is also used regularly. (This modified version has been credited to Heller et al.[19] in [Ref.16] however, the reviewer has not obtained this reference. The citation in this paper is simply a repeat of that found in [Ref.16].)

While the frequency may be predicted "easily," one must know which flow regime to analyze. The regime depends on cavity geometry as well as flow speed. Most recently, it was shown that the boundary layer thickness at the cavity lip is also an important parameter.[6,16] Thus a simulation may be required just to determine the appropriate regime. Moreover, only simulations can predict the amplitude of these tones (both in the near field and in the far field).

Experiments

IN this section, numerous experiments performed over the last fourteen years will be reviewed. Emphasis is placed on simple documentation of both the fluid and cavity parameters for the experiments and the type of data recorded. Mention of experimentally observed physical phenomenon is also made. The experiments discussed in this section have been separated by external flow speed. The past decade saw a renewed effort to understand the fluid-resonant interaction regime because of its relevance to storing and deploying weapons from aircraft weapon bays. Therefore, many of the experiments listed in this section focus on transonic and supersonic flow speeds.

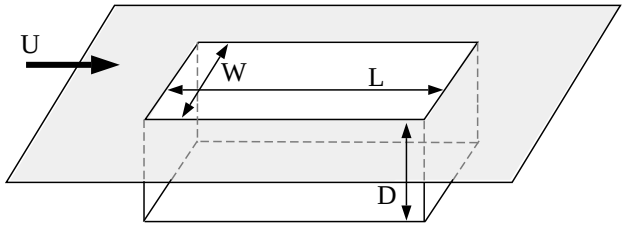

Fig. 3 Cavity geometry and parameters.

Table 1 lists the following parameters (when available) for the experiments discussed in this section: length-to-depth ratio (L/D), width-to-length ratio (W/L); the Mach number of the external flow (M); the Reynolds number (Re) based on cavity length unless otherwise noted; and the boundary layer thickness at the lip of the cavity (δ). The basic cavity geometry is shown in Figure 3. An additional parameter, percent freestream turbulence, appears in the table as well. Not many researchers noted this value, however, when computing flow past a cavity, the flow simulation often depends on this piece of data.

Low Mach number flows

Gharib and Roshko[12] This water tunnel experiment was completed in order to characterize cavity drag for different cavity geometries. During the experiment, at very small L/D the cavity flow did not oscillate. At higher L/D values, only the second and third shear-layer type modes of oscillation were observed. At still higher L/D the cavity shear layer began to stagnate prior to the trailing edge and form a wake mode. Plots of the streamwise velocity profile for the different oscillation conditions are given as well as the Reynolds stress profiles. The coefficient of pressure on the upstream and downstream walls was recorded as well as the drag coefficient. Flow visualization of the shear-layer type oscillation identified two vortical structures within the cavity shear layer when the pressure spectrum was dominated by the second mode and three vortical structures when the third mode dominated.

Erickson and Durgin[18] The interaction between standing waves in a deep cavity and shear-layer instabilities is studied. The interaction takes place through the excitation of the quarter wavelength cavity mode and "lock-on" is demonstrated. The authors show through pressure spectrum at various flow speeds, that the amplitude of the mode increases with Mach num-

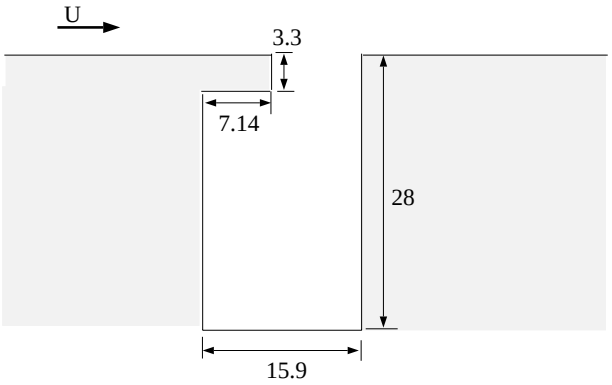

Fig. 4 Geometry for the 3rd CAA workshop category 6.

ber. Flow visualization shows that, at lower velocities, a double vortex structure exists on the interface and at higher velocities only a single vortex structure is formed on the interface.

Disimile et al.[20] This research focused on characterizing the effect of yaw on the cavity flowfield. In order to assess the effect of yaw, zero yaw conditions were also recorded. Pressure time histories along the bottom of the cavity are shown. The upstream boundary layer is analyzed with both its profile and energy spectrum depicted. In addition, the pressure spectrum from a cavity mounted transducer is given. The peak frequencies in the pressure spectrum do not match those predicted by Rossiter's equation (0.1). They do not match the acoustic modes of the cavity either. A discussion on the possible reasons for this disagreement is given in the paper. It is noted that previous studies[21] showed that the Rossiter equation does not predict the peak frequencies for Mach numbers less than 0.2 well.

Henderson[22] As part of the third Computational Aeroacoustics Workshop, Henderson performed experiments that simulated flow past automobile door cavities. Her experimental findings formed the benchmark data for the Category 6 problem. The cavity geometry is shown in Figure 4. The geometry differs from the nominal cavity geometry in that it contains a splitter plate at the front end. The data set consists of SPL values taken at the center left wall (upstream wall). The computational predictions of this flow field are discussed in the next section of this paper.

Zoccola[23] The geometry used by Zoccola also differs from the nominal cavity geometry. In his experiment, the cavity had a top with a slit. The length of this slit was shown to be the important streamwise length parameter (as opposed to the cavity length). The research described in his technical report included measurements of the turbulent boundary layer, shear-layer characteristics, turbulent flow quantities throughout the cavity, and the pressure at the midpoint of the cavity bottom. Shear tones were identified as the speed was increased, with the second mode appearing prior to the first mode. These modes are shown to be well predicted by Nelson's[24] model for flow-excited resonant cavities. (The Nelson model is a kinematic model based on experimental observation.) The changes in the flow field due to passive and active control mechanism are also described.

Jacob et al.[25] A shallow cavity, $L/D = 11$, subject to low-speed flow was investigated in order to better understand the sound generated by the TGV's pantograph casing. Near-field and far-field acoustic measurements were made. The near-field measurements were used for source localization. The results were compared to those from a backward facing step and a wall jet. The cavity pressure spectrum was higher than both. It is shown that the existence of the downstream wall in the cavity amplifies the acoustic field of a backward facing step. Thus the conclusion was made that for such a shallow cavity at low Mach number ($<$ 0.4) and high Reynolds number, the sound radiation is governed by the diffraction of aerodynamical sources by the cavity edges and not by the feed back mechanism.

Jungowski et al.[26] The effect of deep cylindrical cavities as used for side branches in piping systems is explored. A partial review of other research on side branches is included in the introduction of this paper. The paper describes the effect of flow parameters and boundary conditions on the tone generation and tone amplitude in the side branch. The oscillations in the side branch were related to odd multiples of a quarter wavelength. Finally, it was shown that the net acoustic energy radiation or absorption depends on various properties of the flow and acoustics fields and their interaction (i.e. the acoustic field in the main pipe can enhance or suppress the oscillation in the branch significantly). The pressure and velocity amplitude spectrum in the branch end and in the main pipe are shown.

Bruggeman et al.[27,28] The work of Bruggeman also focuses on side branches. However, in both of these papers, the focus is on the use of passive control devices to supress oscillations. In the first, spoilers of different shapes are inserted near the cavity/side-branch lip, and in the latter, grids of louvers are placed across the cavity mouth. In the first, the effect of multiple side branches is also considered. In the second, the effect of louver length and angle is studied as well as the effect of bias flow through the grid. In both articles, the authors compare experimental results to analytical models of the flow field. At the low Mach numbers of interest in these studies, the analytical models based on vortex sound as described by Powell[29] and Howe[30] work quite well to predict the oscillation frequencies and amplitudes. Pressure amplitude in the side branch vs. velocity, frequency, and edge radius are plotted.

Ronneberger[31] The experiments by Ronneberger provide some data for comparison to fluid-elastic in-

teraction predictions. The water tunnel experiments described in Ronneberger's paper show the outcome of forcing the base of the cavity as a piston. The results of flow visualization performed to describe the behavior of the shear layer are presented. In addition, some flow characteristics such as the wall boundary layer profile upstream of the cavity and displacement of the shear layer are reported.

Subsonic, transonic, and supersonic Mach number flows

Gates et al.[32] The experiment described in the Gates et al. paper focuses on parameters which are of relevance to the munitions problem. The cavity model included 33 unsteady pressure transducers and 99 steady pressure transducers. The effect of Mach number, cavity dimension, and blockage were considered. The shallow cavity (L/D=9) supressed tones that existed for the deep cavity configuration (L/D = 4.5). In this work, results for the $L/D = 9$ cavity still showed a tonal nature and thus the cavity was considered transitionally open. The modal frequencies for the deeper cavity followed the modified Rossiter equation (0.2) well ($\kappa = .57$). The amplitude of modes 2 and 3 were the highest for the deeper cavity and mode switching occurred with varying Mach number. It is noted, but not shown, that the modal amplitudes for the shallow cavity do not very with Mach number.

Plentovich[13] Plentovich constructed an experiment in which he could fix the boundary layer thickness at the lip of the cavity but change the Reynold's number and Mach number. Thus he was able to determine that the Reynolds number has little effect on the oscillation frequencies for a subsonic/transonic flow past a cavity. He tested both an L/D that should give open cavity flow and one that should give closed cavity flow based on previous reports. He was able to show that the "criterion" for open/closed does not only depend upon the geometry of the cavity (L/D) but also on the flow Mach number. Several data sets of the static pressure along the cavity walls are given in this technical report. Using these data, Plentovich characterized the various geometry and Mach number combinations as open/closed/transitional. These pressure profiles indicated that the pressure in the aft part of a shallow cavity is sensitive to the boundary layer thickness.

Tracy and Plentovich[1633] This set of technical reports provides wall pressure data for a wide range of cavity geometries and Mach numbers. Again the point is made, that the flow nature (open/transitional/closed) is dependent upon the Mach number. The tones that are present are shown to be in good agreement with the modified Rossiters equation (0.2). The research shows that the Reynolds number does not affect tone amplitude or bandwidth but Mach number does. The cavities they tested do not all produce tones at all of the Mach numbers investigated. The reason for the "disappearance" of tones is not entirely clear in all cases. For instance, at M = 0.2, $L/D = 4.4$ and 6.7 no tone is produced. However the experiments of Ahuja and Mendoza[6] for a similar flow/cavity configuration do produce a tone. This discrepancy could be related to a difference in the boundary layer thickness of the two experiments.

Ahuja and Mendoza[6] An extensive data set was generated to allow for validation of computational acoustic codes. Numerous velocity spectra and pressure spectra plots are provided in this contractor's report. A test for the effect of span on the cavity centerline measurements shows that for L/W > 1 these effects are important. As with all of the other experimental investigations, it was shown that the 2nd and 3rd modes dominate the spectrum and that the Reynolds number has no affect on the tone. A boundary layer study showed that for δ/L greater than .7, all tones are eliminated. (Others have shown a similar dependence on δ/D.[33]) The disturbance convection velocity was measured as roughly 60% to 65% of the freestream which is slightly higher than that found earlier by Rossiter. Acoustic measurements were made outside of the cavity. The pressure spectrum at the point directly above the middle of the cavity is given for various flow/cavity configurations. The pressure directivity of the dominant mode is also given for some geometries. The directivity of the acoustic field surrounding a shallow cavity is shown to be flat while that about a deeper cavity showed a directional preference dowstream. For the shallow cavities at transonic speeds there was no suppression of the tones apparent. In addition, at low Mach number for shallow cavities there was no evidence of a wake mode.

Cattafesta et al.[34] This study attempts to explain additional low frequency peaks in cavity flow spectrum (not Rossiter modes). Also discussed is the reason for the mode-switching phenomenon. All of these effects are attributed to nonlinear interactions. In particular the authors show that for a cavity with L/D = 2 at a Mach number of 0.4, the nonlinearities are strong, while for a cavity with $L/D = 4$ at M = 0.6 they are almost nonexistent. The authors propose that when three Rossiter modes are present such that ($f_c > f_b > f_a$) with $f_c - (f_a + f_b) \approx 0$, significant nonlinear coupling occurs "leading to a low-frequency amplitude modulation of the primary modes." They compute the Rossiter modes using $\alpha = 0.25, \kappa = 0.66$. The peak Strouhal numbers for the two cavities at varying Mach number are given. In addition, the pressure spectrum measured at the upstream cavity wall is shown for the two cases mentioned above.

Shaw et al.[35] Experiments were performed on a scaled model of the F-111 with weapons bay. The effect of two leading edge spoiler devices was analyzed. Four transducers in the cavity were used to record pressure. A comparison between the peaks in

the pressure spectrum for one of the cases and modes computed using the modified Rossiter's equation with ($\alpha = 0.57, \kappa = 0.64$) shows good agreement. However, it is not clear if the comparison is made for the shallow or deep cavity nor whether the spoiler is included or not. In addition, there is no explanation concerning the choice of α accept that it is dependent upon L/D. The authors compare the experimental findings to flight test data as well as the modified Rossiter's equation with the parameters given by Rossiter. The prediction and wind tunnel data compare well, however, they do not match the flight test data.

McGrath and Shaw[36] This article also focuses on the effect of control devices on the tones produced by transonic flows past weapons bays. Here an oscillating flap at the leading edge and a high frequency tone generator are considered. The tones measured for the case of no control at supersonic Mach number compare well to predictions made with Rossiter's equation while tones for subsonic Mach numbers do not. The paper contains tables of the dominant mode (two) frequencies for the cases with and without control. Pressure spectrum for the various flow/geometry configurations are provided and prove the ability of the control devices to suppress the tones.

Raman et al[17] The authors consider a jet-cavity setup. They show that the presence of the cavity changes the tonal nature of the jet and vice versa. That is, "the jet-cavity interaction produces a unique set of tones." They investigate two cavity geometries, one of $L/D = 3$ and the other with $L/D = 8$. They, like Plentovich[13] show that the characterization of these cavities as open, transitional, or closed actually depends upon the Mach number. The tones that they find for the deeper cavity do not follow those predicted by Rossiters equation. Instead they find that $f = \frac{U}{L}\frac{.3m}{\sqrt{M}}$ for the deep cavity and $f = \frac{c_0}{L}\frac{m+1}{4}$ for the shallow cavity. Here U and M refer to the jet exit flow velocity. Thus they found that the tones for the shallow cavity depend on the acoustic modes of the cavity and not on the flow, while the deeper cavity tones depended significantly on the flow. This is in contrast to other experimental findings where moderately shallow cavities were excited at the depth mode[6] and where deeper cavities have exhibited "lock on" at the cavity depth mode. The article provides flow visualization, tone frequency plots, tone amplitude plots, and maps of the nearfield unsteady pressure. The authors also state that the pressure on the cavity floor provides very little insight about the resonant tones.

Dix and Bauer[14] The Air Force's WICS database created at the Arnold Engineering Development Center is partially presented in this work. The experiments provide pressure spectrum from transducers on the cavity floor and the upstream and downstream faces. Some transducers were placed off center in order to quantify three-dimensional effects. The convection speed of disturbances was measured to be between 60 and 70% of the freestream which is higher than that reported by Rossiter. Also, the parameter α in Rossiter's formula is given as a function of L/D: $\alpha = 0.062\frac{L}{D}$. Using these values, the first 4 modes match those predicted by Rossiters equation. The off-center data provide evidence of the existence of "lateral pressure gradients attributed to acoustic waves crossing the cavity in the vertical direction."

Computations

ADVANCES in computational capabilities continually occur and have impacted the prediction of cavity response to grazing flow. Komerath et al.[9] mention some early computational work in their 1987 review article. Many articles cited in [Ref.9] performed inviscid flow simulations for very low Mach number flows with the exception of the work by Hankey and Shang.[37] Now, one generally expects cavity flow simulations to account for viscous effects and turbulence (when appropriate).

Table 3 lists numerous references that describe computational simulations of cavity flow. Several categories of simulation exist. For low Mach number simulations, researchers have coupled inviscid acoustic field equations with simulations of the viscous, incompressible, Reynolds Averaged Navier Stokes (RANS) simulations.[1–4] For subsonic, transonic, and supersonic Mach numbers researchers have solved the compressible RANS equations.[5,15,38–47] A few have solved the mass averaged Navier Stokes (MANS) equations.[48,49] For supersonic flow speeds, some have chosen to use the double thin-layer Navier Stokes formulation.[50,51] A new LES/RANS approach[52] was introduced recently and a direct numerical simulation has been completed.[53]

Table 3 has been organized first according to Mach number of the reported simulation, second by whether the simulation was two-dimensional or three-dimensional, and third by flow solver type. For each reference, the Mach number, length-to-depth ratio (L/D), Reynolds number based on length, and solution type 2D or 3/D are specified. An additional column indicates whether the results have been validated using experimental data and gives the appropriate reference. Many of the references are discussed in either the previous section of this paper or [Ref.9]. However, the current author did not obtain a few of the technical reports, and thus the citation from the referring article is simply repeated in this paper. The final column summarizes the basic fluid dynamic model used for the simulation. A key for the abbreviations used in the table proceeds the table.

Inviscid Simulation At low Mach number and high Reynolds number, if one is interested in predicting the frequency, and approximating the amplitude, of the

unsteady cavity oscillations, boundary element potential flow simulations can be used. Kriesels et al.[54] showed that a panel type method can simulate well flow past an open cavity when one accounts for the separation from the cavity leading edge (through the use of a kutta type condition) and allows the vortex sheet simulating the shear layer to evolve freely.

Viscous/Acoustic splitting techniques Four methods are described in which a viscous, incompressible, RANS solution of the near-field unsteady flow field is coupled to a governing set of equations for the acoustic field. Such methods are valid for low Mach number flows where the time necessary for the acoustic pulse that emanates from the trailing edge to travel up to the leading edge is negligible. These methods explicitly address the computation of the acoustic field surrounding the cavity.

- Hardin and Pope[1] solve for the incompressible, viscous fluid dynamics by solving the stream function equation coupled to the Poisson equation for hydrodynamic pressure. The known hydrodynamic flow parameters then are U, V, and P. They then define the hydrodynamic density as

$$\rho_1 = \frac{P - \bar{P}}{c_0^2}$$

  where c_0 is the speed of sound and the bar indicates mean value. The acoustic field quantities are introduced then as corrections to the hydrodynamic field. That is,

$$u = U + u'$$

$$v = V + v'$$

$$p = P + p'$$

$$\rho = \rho_0 + \rho_1 + \rho'$$

  However, the existence of a fluctuating density field for an incompressible flow seems contradictory. They then derive a set of governing differential equation for the acoustic quantities coupling them to the hydrodynamic quantities. They solve the acoustic equations using a MacCormack scheme. A characteristic type boundary condition is used at the open domain boundaries.

- Moon et al.[3] also apply the acoustic quantity derivation of Hardin and Pope. However, they solve for the incompressible, viscous field, "using a projection method based algorithm called SMAC (Simplified Marker and Cell)[55]" (which is unfamiliar to the current author).

- Slimon et al.[4] use a method whose foundation is similar to that Hardin and Pope. They call their method EIF (expansion about incompressible flow) and define their hydrodynamic density as

$$\frac{D\rho_1}{Dt} = M^2 \frac{DP}{Dt}$$

  Simulation of the incompressible, viscous flow allows for turbulence. They solve the unsteady RANS equations using central finite differencing in space and Runge Kutta in for the time integration. Second and fourth order dissipation is added. The turbulence modeling method of Moore and Moore[56] is used. The acoustic equations are solved using the MacCormack scheme with explicit time integration. The open domain boundaries are treated with the perfectly matched layer (PML).[57]

- Grace and Curtis[2,58] also solve for the incompressible, viscous flow field as a first step. However, they couple this to an appropriate form of the governing wave equation to solve for the acoustic field. In the limit of vanishing Mach number, the governing acoustic equation takes a form similar to Lighthill's equation. Other forms of the equation valid for low subsonic Mach number are given in Goldstein's book.[59] The viscous (laminar) flow field was computed using OVERFLOW which is a finite difference RANS simulation[2] and FLUENT which is a finite volume RANS simulation.[58] The acoustic equation is solved using a simple second order finite difference discretization in space and time. The radiation boundary condition of Hagstrom and Hariharan[60] are used at open domain boundaries. The source term that forces the acoustic equation is computed at every time step using the incompressible viscous flow results.

Third CAA workshop on benchmark problems Category 6 of the third CAA workshop on benchmark problems required the calculation of the frequency and sound pressure level of tones associated with the flow of air over an automobile door gap cavity. However, the experiments did not include any field pressure measurements (only a cavity-wall pressure transducer was used). Therefore, the assessment of the acoustic predictive capabilities of a code cannot be fully analyzed using the available data for this problem. Four computational simulations were attempted for this problem.[3,38,39,61] None were able to simulate the amplitude of the pressure on the upstream vertical cavity wall measured in the experiment. Several[3,38,39] were able to estimate the frequency of the main oscillation mode. The four methods used to compute this flow field differed. Kubotskii and Tam[38] and Sheih and Morris[61] used the DRP (dispersion relation preserving) scheme[62] with artificial damping to discretize the Navier Stokes

equation. Ashcroft et al.[39] used the NASA CFL2D code which is a basic finite volume RANS code utilizing second order central differencing in space and the flux splitting of Roe. Finally, Moon et al.[3] used a viscous/acoustic type computation described above.

Telescope Cavity The Boeing 747-SP houses the Stratospheric Observatory for Infrared Astronomy (SOFIA) in an open cavity. Srinivasan[63] cites several experiments and computational investigations which have been performed to better understand the SOFIA cavity environment. Srinivasan performed a three-dimensional simulation of the flow field using the RANS code OVERFLOW, a finite different code which uses a central difference scheme with second and fourth order numerical dissipation. The Baldwin Lomax turbulence model is used above horizontal walls while the shear-layer model implemented within OVERFLOW[64] is used inside the cavity. The computed time averaged results match experimental data well and the sound pressure spectrum is in general agreement with the flight test data. For this same application, Venkatapathy[47] focused on using two-dimensional simulations to fully study the effect of the contoured cavity shape and the effect of lip blowing to control the flow field. The computational model solved the Navier Stokes using the "Conservative Supra Characteristic Method[65]" (which is unfamiliar to the present reviewer).

Colonius et al.[53] Colonius et al. use DNS for the entire flowfield. They employ a 6th order compact finite difference scheme in space and an explicit fourth order Runge Kutta time integration. They consider two geometries and capture both shear and wake modes respectively.

Others The total variation diminishing (TVD) scheme of Chakravarthy[66] has been used by Gorski and Ota[45] and Dougherty et al.[42] Both simulations implemented a form of the Baldwin-Lomax turbulence model and the latter was able to match the frequencies predicted by Rossiter by forcing the boundary layer thickness at the cavity lip to match those in Rossiter's experiment. Zhang[48] solves the MANS equations using a finite volume approach with a $k-\omega$ turbulent model corrected for compressibility. The solutions are compared to data taken previously by Zhang. Shih et al. utilize a formulation for the MANS strongly coupled to a two-equation turbulence model[67] to study transonic flow past a transitional cavity. The mean wall pressure results compare favorably with experiment. Kim and Chokani[68] studied passive control devices using a RANS simulation with a two layer algebraic turbulence model due to Cebeci and Smith.[69] The time dependent wall pressure calculated using this method matched experimental data very well.

Turbulence Modeling

Shieh and Morris[5,40] Sheih and Morris have developed a computational method for computational acoustics and have recently applied it to flow past a cavity. Their method embeds into a parallel RANS simulation the one-equation Spalart-Allamaras turbulence model[70] and the detached eddy simulation (DES) method of Spallart et al.[71] They use the DRP scheme of Tam and Web[62] for spatial discretization and explicit fourth order Runge Kutta integration in time. They solve for two-dimensional flow past two different geometries. One shows the characteristics of oscillations due to a shear-layer mode and the other operates in the wake mode. It is noted that the geometry, which in simulation responds in a wake mode, does not respond as such experimentally (however the cavity is three-dimensional in experiments). The simulations show a disturbance convection speed of 0.25 U for the wake mode and comparisons of the tones produced with those predicted by Rossiter's equation ($\kappa = 0.25$) give good agreement. The article includes pressure contours away from the cavity. The field pressure has a peak radiation at 135° measured from the downstream axis for a flow Mach number of 0.6. The simulations show that the directivity is the same for both cavity modes. The magnitude of the peak radiation is higher for the wake mode.

Baysal[15,46,72–74] Baysal has been active in the computation of transonic flows past cavities. He usually solves the RANS equations using a finite volume approach with fourth order damping. The key to his computational successes seems to be his turbulence model which is a modified Baldwin-Lomax model. The modifications account for "vortex-boundary layer interaction and separation, multiple walls, and turbulent memory effects".[15]

Tam et al.[51,75] Tam, Orkwis, and Disimile use a finite volume solution of the double thin-layer Navier Stokes equation to simulate supersonic flow past a cavity. In their first paper, they compare results obtained using Baldwin-Lomax models previously implemented by other researchers. For instance: Suhs[50] applied the standard Baldwin-Lomax model above horizontal walls and assumed laminar flow in the cavity; Rizzetta[49] (and Tu[76]) used a modified model that included a relaxation (or memory) model; Degani and Schiff added the first peak modification and the multiple wall modification. For supersonic flow past an open cavity, the standard Baldwin-Lomax was the most dissipative (even more than a fully laminar simulation). The article also shows, that while each model has its strength, none performed consistently well across the entire cavity. In the second paper, they adopt the turbulence model of Baysal which includes "the upstream relaxation, multiple walls, and first peak modifications". With this turbulence model and the DTNS simulation they were able to reproduce qualitatively the supersonic flow field past an open cavity.

Fuglsang and Cain[43] Fuglsang and Cain offer yet another approach to the modeling of turbulence for the cavity geometry. They use the Baldwin-Lomax

turbulence model upstream but then apply DNS in the cavity region. They focus their simulation on assessing the effect of forcing the shear layer.

CRAFT The CRAFT code has been developed by researchers at Combustion Research and Flow Technology Inc. They have tested this code on the problem of transonic and supersonic flow past cavities.[44,52,77] A table of the code's features is given in Sinha et al.[44] The code has been created to solve either a large eddy simulation (LES) or a RANS simulation. In trying to apply the solver to the cavity flow problem, the developers tested numerous turbulence models including a $k-\epsilon$ formulation and an LES formulation.[44] Later, they employed a hybrid model of $k-\epsilon$ and $k-\omega$ called $k-kl$.[52] With this latest scheme they were better able to model the flow physics. The CRAFT code with yet another turbulence model modification has been used to model both cavity and store. The paper by Stanek et al.[77] includes a short review of experimental and computational findings for weapons bay applications as well as a simulation using the CRAFT code.

Summary

IT has been shown in this article that a greater understanding of the flow field and acoustic field generated by grazing flow past a cavity has been gained over the past ten years. In addition, CFD is becoming a more reliable prediction tool for this flow field. Many CFD analyses described in this report rely on a modified Baldwin Loman turbulence model to correctly simulate the shear layer in turbulent flow conditions.

As more confidence is gained in the use of CFD as a methodology for the prediction of such complicated phenomenon such as flow past cavities, more researchers are using this method to study the effect of control devices and cavity/body interactions. Some of the papers mentioned in this article attempt to elucidate the difference between flow fields when either passive or active control devices are present.[46,50,52,68,77] In addition, some research reviewed here (applicable to the weapons bay problem) included the munition in the model.[74,77]

Few researchers have attempted to incorporate acoustic field calculations into their predictions. The methods used by those who have focused on the acoustic field have been briefly described in this paper. It is obvious that more work is needed in this area. The grid stretching normally used in the CFD simulations to decrease grid boundary reflections often distorts the acoustic field. Thus hybrid CFD/acoustic methods or CAA methods must still be refined for the acoustic field prediction of cavity flow.

References

[1]Hardin, J. C. and Pope, D. S., "Sound Generation by Flow over a Two-Dimensional Cavity," *AIAA Journal*, Vol. 33, No. 3, March 1995, pp. 407–412.

[2]Grace, S. M. and Curtis, C. K., "Acoustic Computations Using Incompressible Inviscid CFD Results as Input," *NCA-Vol 26, Proceedings of the ASME Noise Control and Acoustics Division*, 1999, pp. 103–108.

[3]Moon, Y. J., Koh, S. R., Cho, Y., and Chung, J. M., "Aeroacoustic Computations of the Unsteady Flows Over a Rectangular Cavity with a Lip," *Third Computational Aeroacoustics Workshop on Benchmark Problems*, edited by M. D. Dahl, Ohio Space Institute, NASA/CP-2000-209790, 2000, pp. 355–361.

[4]Slimon, S. A., Davis, D. W., and Wagner, C. A., "Far-field Aeroacoustic Computation of Unsteady Cavity Flows," *AIAA Paper No., 98-0285*, 1998.

[5]Shieh, C. M. and Morris, P. J., "Parallel Computational Aeroacoustic Simulation of Turbulent Subsonic Cavity Flow," *AIAA Paper No. 2000-1914*, 2000.

[6]Ahuja, K. K. and Mendoza, J., "Effects of Cavity Dimensions, Boundary Layer and Temperature on Cavity Noise with Emphasis on Benchmark Data to Validate Computational Aeroaoucstic Codes," Tech. Rep. NAS1-19061, Task 13, NASA Contractor Report: Final Report, 1995.

[7]Heller, H. H. and Bliss, D. B., "Aerodynamically Induced Pressure Oscillations in Cavities–Physical Mechanisms and Suppression Concepts," Tech. Rep. AFFDL-TR-74-133, 1975.

[8]Rockwell, D. and Naudascher, E., "Self-Review – Sustained Oscillations of Flow Past Cavities," *Journal of Fluids Engineering*, Vol. 100, june 1978.

[9]Komerath, N. M., Ahuja, K. K., and Chambers, F. W., "Prediction and Measurement of Flow Over Cavities-A Survey," *AIAA Paper No. 87-0166*, 1987.

[10]Sarohia, V., "Experimental Investigation of Oscillations in Flows Over Shallow Cavities," *AIAA Journal*, Vol. 15, No. 7, 1977.

[11]Rossiter, J. E., "Wind-tunnel Eexperiments on the Flow Over Rectangular Cavities at Subsonic and Transonic Speeds," Tech. Rep. Reports and Memo No. 3438, Aeronautical Research Council, 1966.

[12]Gharib, M. and Roshko, A., "The Effect of Flow Oscillations on Cavity Drag," *Journal of Fluid Mechanics*, Vol. 177, 1987, pp. 501–530.

[13]Plentovich, E., "Three-dimensional Cavity Flow Fields at Subsonic and Transonic Speeds," Tech. Rep. TM 4209, NASA Langley Research Center, 1992.

[14]Dix, R. E. and Bauer, R. C., "Experimental and Predicted Acoustic Amplitutdes in a Rectangular Cavity," *AIAA Paper No. 2000-0472*, 2000.

[15]Srinivasan, S. and Baysal, O., "Navier-Stokes Calculations of Transonic Flow Past Cavities," *Journal of Fluids Engineering*, Vol. 113, September 1991, pp. 369–376.

[16]Tracy, M. B. and Plentovich, E., "Measurements of Fluctuating Pressure in a Rectangular Cavity in Transonic Flow at High Reynolds Numbers," Tech. Rep. TM 4363, NASA Langley Research Center, 1992.

[17]Raman, G., Envia, E., and Bencic, T. J., "Tone Noise and Nearfield Pressure Produced by Jet-Cavity Interaction," Tech. Rep. TM-1998-208836, AIAA Paper No, 99-0604, NASA Lewis Research Center, 1998.

[18]Erickson, D. D. and Durgin, W. W., "Tone Generation by Flow Past Deep Wall Cavities," *AIAA Paper No. 87-0167*, 1987.

[19]Heller, H. H., Holmes, G., and Covert, E. E., "Flow-Induced Pressure Oscillations in Shallow Cavities," Tech. Rep. AFFDL-TR-70-104, 1970. (Available from DTIC as AD 880 496).

[20]Disimile, P. L., Toy, N., and E, S., "Pressure Oscillations in a Subsonic Cavity at Yaw," *AIAA Journal*, Vol. 36, No. 7, July 1998, pp. 1141–1148.

[21]Tam, C. K., "The Acoustic Modes of a Two-dimensional Rectangular Cavity," *Journal of Sound and Vibration*, Vol. 49, No. 3, 1976, pp. 353–364.

[22]Henderson, B., "Automobile Noise Involving Feedback-Sound Generation by Low Speed Cavity Flows," *Third Computational Aeroacoustics Workshop on Benchmark Problems*, edited by M. D. Dahl, Ohio Space Institute, NASA/CP-2000-209790, 2000, pp. 95–100.

[23]Zoccola, P. J., *Experimental Investigation of Flow-Induced Cavity Resonance*, Ph.D. thesis, Catholic University of America, Washington D. C., 2000.

[24]Nelson, P. A., Halliwell, N. A., and Doak, P. E., "Fluid Dynamics of a Flow Excited Resonance, Part II: Flow Acoustic Interaction," *Journal of Sound and Vibration*, Vol. 91, 1983, pp. 375–402.

[25]Jacob, M. C., Gradoz, V., Louisot, A., Juve, D., and Guerrand, S., "Comparison of Sound Radiation by Shallow Cavities and Backward Facing Steps," *AIAA Paper No. 99-1892*, 1999.

[26]Junbgowski, W. M., Botros, K. K., Studzinski, W., and Berg, D. H., "Tone Generation of Flow Past Confined, Deep Cylindrical Cavities," *AIAA Paper No. 87-2666*, 1987.

[27]Bruggeman, J. C., Hirschberg, A., van Dongen, M. E. H., Wijnands, A. P. J., and Gorter, J., "Self-sustained Aero-acoustic Pulsations in Gas Trans port Systems: Experimental Study of the Influence of Closed Side Branches," *Journal of Sound and Vibration*, Vol. 150, No. 3, 1991, pp. 371–393.

[28]Bruggeman, J. C., Vellekoop, J. C., van der Knapp, F. G. P., and Keuning, P. J., "Flow Excited Resonance in a Cavity Covered by a Grid: Theory and Experiments," *NCA Vol 11. FED-Vol. 130, Flow Noise Modeling, Measurement and Control*, 1991, pp. 135–144.

[29]Powell, A., "Theory of Vortex Sound," *Journal of the Acoustical Society of America*, Vol. 35, No. 1, 1964, pp. 177–195.

[30]Howe, M. S., "Contributions to the Theory of Aerodynamic Sound with Applications to Excess Jet Noise and the Theory of the Flute," *Journal of Fluid Mechanics*, Vol. 71, No. 4, 1975, pp. 625–273.

[31]Ronneberger, D., "The Dynamics of Shearing Flow Over a Cavity-A Visual Study Related to the Acoustic Impedance of Small Orifices," *Journal of Sound and Vibration*, Vol. 71, No. 4, 1980, pp. 565–581.

[32]Gates, R. S., B.Butler, C., Shaw, L. L., and Dix, R. E., "Aeroacoustic Effects of Body Blockage in Cavity Flow," *AIAA Paper NO. 87-2667*, 1987.

[33]Tracy, M. B. and Plentovich, E., "Characterization of Cavity Flow Fields Using Pressure Data Obtained in the Langley 0.3-Meter Transonic Cryogenic Tunnel," Tech. Rep. TM 4436, NASA Langley Research Center, 1993.

[34]Cattafesta III, L. N., Garg, S., Kegersie, M. S., and Jones, G. S., "Experiments on Compressible Flow Induced Cavity Oscillations," *AIAA Paper No,. 98-2912*, 1992.

[35]Shaw, L., Clark, R., and Talmadge, D., "F-111 Generic Weapons Bay Acoustic Environment," *AIAA Paper No.87-0168*, 1987.

[36]McGrath, S. and Shaw, L., "Active Control of Shallow Cavity Acoustic Resonance," *AIAA Paper No. 96-1949*, 1996.

[37]Hankey, W. L. and Shang, J. S., "Analyses of Pressure Oscillations in an Open Cavity," *AIAA Journal*, Vol. 18, No. 1, August 1980, pp. 892–898.

[38]Kurbatskii, K. K. and Tam, C. K., "Direct Numerical Simulation of Automobile Cavity Tones," *Third Computational Aeroacoustics Workshop on Benchmark Problems*, edited by M. D. Dahl, Ohio Space Institute, NASA/CP-2000-209790, 2000, pp. 371–382.

[39]Ashcroft, G. B., Takeda, K., and Zhang, X., "Computations of Self-Induced Oscillatoroy Flow in an Automobile Door Cavity," *Third Computational Aeroacoustics Workshop on Benchmark Problems*, edited by M. D. Dahl, Ohio Space Institute, NASA/CP-2000-209790, 2000, pp. 355–361.

[40]Shieh, C. M. and Morris, P. J., "Parallel Numerical Simulation of Subsonic Cavity Noise," *AIAA Paper No. 99-1891*, 1999.

[41]Atwood, C., "Computation of a Controlled Store Separation from a Cavity," *Journal of Aircraft*, Vol. 32, No. 4, July-August 1995, pp. 846–852.

[42]S.Dougherty, N., Holt, J. B., Nesman, T. E., and Farr, R. A., "Time-Accurate Navier-Stokes Computations of Self-Excited Two-Dimensional Unsteady Cavity Flows," *AIAA Paper No. 90-0691*, 1990.

[43]Fuglsang, D. and Cain, A. B., "Evaluation of Shear Layer Cavity Resonance Mechanisms by Numerical Simulation," *AIAA Paper No. 92-0555*, 1992.

[44]Sinha, N., Dash, S. M., Chidambaram, N., and Findlay, D., "A Perspective on the Simulation of Cavity Aeroacoustics," *AIAA Paper No. 98-0286*, 1998.

[45]Gorski, J., Ota, D. K., and Chakravarthy, R., "Calculation of Three-Dimensional Cavity Flowfields," *AIAA Paper No. 87-0117*, 1987.

[46]Baysal, O., Yen, G.-W., and Fouladi, K., "Navier-Stokes Computations of Cavity Aeroacoustics with Suppression Devices," *Journal of Vibration and Acoustics*, Vol. 116, January 1994, pp. 105–112.

[47]E.Venkatapathy, Lombard, C. K., and Nagaraj, N., "Numerical Simulation of Compressible Flow Around Complex Two-Dimensional Cavities," *AIAA Paper No. 87-0116*, 1987.

[48]Zhang, X., "Compressible Cavity Flow Oscillation due to Shear Layer Instabilities and Pressure Feedback," *AIAA Journal*, Vol. 33, No. 8, August 1995, pp. 1404–1411.

[49]Rizzetta, D., "Numerical Simulation of Supersonic Flow Over a Three-Dimensional Cavity," *AIAA Journal*, Vol. 26, No. 7, July 1988, pp. 799–807.

[50]Suhs, N. E., "Unsteady Flow Computations for a Three-dimensional Cavity with and without an Acoustic Supression Device," *AIAA Paper No. 93-3402-CP*, 1993.

[51]Tam, C.-J., Orkwis, P. D., and Disimile, P. J., "Algebraic Turbulence Model Simulations of Supersonic Open-Cavity Flow Physics," *AIAA Journal*, Vol. 34, No. 11, November 1996, pp. 2255–2260.

[52]Arunajatesan, S., Sinha, N., and Menon, S., "Towards Hybrid LES-RANS Computations of Cavity Flowfields," *AIAA Paper No. 2000-0401*, 2000.

[53]Colonius, T., Basu, A. J., and Rowley, C. W., "Numerical Investigatino of the Flow Past a Cavity," *AIAA Paper No. 99-1912*, 1999.

[54]Kriesels, P. C., Peters, M. C. M., Hirschberg, A., Wijnands, A. P. J., Iafrati, A., Riccardi, G., Piva, R., and Bruggeman, J. C., "High Amplitude Vortex-Induced Pulsations In A Gas Transport System," *Journal of Sound and Vibration*, Vol. 184, No. 2, 1995, pp. 343–368.

[55]Hirt, C. W. and Cook, J. L., "Calculating Three-Dimensional Flows around Structures and over Rough Terrain," *Journal of Computational Physics*, Vol. 10, 1972, pp. 324–340.

[56]Moore, J. G. and Moore, J., "Controlling Over-production of Turbulence in Two-Equation Models by Lmiting Anisotropy of the Reynolds Normal Stresses," *ASME FED Paper FEDSM97-3356*, 1997.

[57]Hu, F. Q., "On Absorbing Boundary Conditions for Linearized Euler Equations by a Perfectly Matched Layer," *Journal of Computational Physics*, Vol. 129, No. 1, November 1996, pp. 201–219.

[58]Granda, C. K., *A Computational Acoustic Prediction Method Applied to Two-Dimensional Cavity Flow*, Master's thesis, Boston University, Boston, MA, to appear in February 2001.

[59]Goldstein, M. E., *Aeroacoustics*, McGraw-Hill International Book Co., New York, etc., 1976, pp. 249–254.

[60]Hagstrom, T. and Hariharan, S. I., *Progressive Wave Expansions and Open Boundary Problems*, Vol. 86, Springer Verlag, 1996, pp. 23–43.

[61]Shieh, C. W. and Morris, P. J., "A Parallel Numerical Simulation of Automobile Noise Involving Feedback," *Third Computational Aeroacoustics Workshop on Benchmark Problems*,

edited by M. D. Dahl, Ohio Space Institute, NASA/CP-2000-209790, 2000, pp. 363–370.

[62]Tam, C. K. W. and Web, J. C., "Dispersion-relation-preserving Finite Difference Schemes for Computational Aeroacoustics," *Journal of Computational Physics*, Vol. 107, 1993, pp. 262–281.

[63]Srinivasan, G. R., "Acoustics and Unsteady Flow of Telescope Cavity in an Airplane," *Journal of Aircraft*, Vol. 37, No. 2, March-April 2000, pp. 274–281.

[64]Bunign, P. G. and Chan, W. M., "OVERFLOW User's Manual, Version 1.7u," Tech. rep., NASA Ames Research Center, 1997.

[65]Lombard, C. K., Bardina, J., Venkatapathy, E., and Oliger, J., "Multi-Dimensional Formulation of CSCM- An Upwind Flux Difference Eigenvector Split Method for the Compressible Navier Stokes Equations," *AIAA Paper No. 83-1895*, 1983.

[66]Chakravarthy, S. R. and Osher, S., "A New Class of High Accuracy TVD Schemes for Hyperbolic Conservation Laws," *AIAA Paper No. 85-0363*, 1985.

[67]Nichols, R. H., "A Two-Equation Model for Compressible Flows," *AIAA Paper No. 90-0494*, 1990.

[68]Kim, I. and Chokani, N., "Navier-Stokes Study of Supersonic Cavity Flowfield with Passive Control," *Journal of Aircraft*, Vol. 29, No. 2, March-April 1992, pp. 217–223.

[69]Shang, J. S. and Hankey Jr., W. L., "Numerical Solutiosn for Supersonic Turbulent Flow over a Compression Ramp," *AIAA Journal*, Vol. 13, 1975, pp. 1368–1374.

[70]Spalart, P. R. and Allmaras, R. S., "A One-equation Turbulence Model for Aerodynamic Flows," *AIAA Paper No. 92-04393*, 1992.

[71]Spalart, P. R., Jou, W. H., Streles, M., and Allamaras, S. R., "Comments on the Feasibility of LES for wings and on a Hybrid RANS/LES Approach," *Proceedings of the first AFOSR International Conference on DNS/LES*, Greydon Press, Columbus, OH, 1997.

[72]O.Baysal and Stallings Jr., R. L., "Computational and Experimental Investigation of Cavity Flowfields," *AIAA Paper No. 87-0114*, 1987.

[73]Baysal, O. and Stallings Jr., R. L., "Computational and Experimental Investigation of Cavity Flowfields," *AIAA Journal*, Vol. 26, No. 1, January 1988, pp. 6–7.

[74]Baysal, O., Fouladi, K., Leung, R., and Sheftic, J. S., "Interference Flows Past Cylinder-Fin-Sting-Cavity Assemblies," *Journal of Aircraft*, Vol. 29, No. 2, March-April 1992, pp. 194–202.

[75]Tam, C.-J. and Orkwis, P. D., "Comparison of Baldwi-Lomax Turbulence Models for Two-Dimensional Open Cavity Computations," *AIAA Journal*, Vol. 34, No. 3, 1996, pp. 629–631.

[76]Tu, Y., "Unsteady Navier Stokes Simulations of Supersonic Flow Over a Three-Dimensional Cavity," *AIAA Paper No. 92-2632-CP*, 1992.

[77]Stanek, M. J., Sinha, N., Ahuja, V., and Birkbeck, R. M., "Acoustics-compatible Active Flow Control for Optimal Weapon Separation," *AIAA Paper No. 99-1911*, 1999.

[78]Rossiter, J. E., "The Effect of Cavities on the Buffeting of Aircraft," Tech. Rep. 754, Royal Airface Establishment, 1962.

[79]Shih, S. H., Hamed, A., and Yeuan, J. J., "Unsteady Supersonic Cavity Flow Simulations Using Coupled κ-ϵ and Navier-Stokes Equations," *AIAA Journal*, Vol. 32, No. 10, October 1994, pp. 2015–2021.

[80]II, L. G. K., Maciulaitis, A., and Clark, R. L., "Mach 0.6 to 3.0 Flows over Rectangular Cavities," Tech. Rep. AFWAL-TR-82-3112, Air Force Wright Aeronautical Labs, 1983.

[81]Dix, R. E. and Dobson Jr., T. W., "Database for Internal Store Carriage Jettison," Tech. Rep. AEDC-TR-90-23 vols. 1,2, USAF Arnold Engineering and Development Center, 1990.

[82]Crosby, W. A., Carman, J. B., Hawkins, W. R., and Simons, S. A., "Store Separation Tests at Supersonic Speeds from Internal Carriage Position of a Generic Weapons Bay," Tech. Rep. AEDC-TSR-88-V9, TN, USAF Arnold Engineering and Development Center, 1988.

Key for the Table 3.

NS	Navier Stokes
RANS	Reynolds averaged NS
IRANS	incompressible RANS
MANS	Mass averaged NS
LES	large eddy simulation
DNS	direct numerical simulation
DES	detached eddy simulation
DTNS	double thin-layer NS
DRP	dispersion relation preserving
TVD	total variation diminishing
BL	Baldwin Lomax
SpAl	1-eq. Spallart and Allamaras
MM	tested multiple turbulence models
BL mod	modified BL (no all modifications are the same)
LA	Lighthill's acoustic analogy
Same	experiment described in same reference
Priv.	internal technical report (see referring paper for details)
SOFIA	experiments related to SOFIA project given in [Ref.63]

Ref.	M	L/D	W/L	Re_L	Lam/Turb	δ/L	Turb. int.
Gharib and Roshko[12]	$\sim$ .002	0.6 $\rightarrow$ 1.2	axisym	6×10^5	L	$\sim$ 0.007	0.05%
Erickson and Durgin[18]	0.09, 0.18, 0.24	0.05, 0.16	1	1×10^5	NG	NG	NG
Disimile et al.[20]	0.04	1	8.7	8.48×10^4	T	2.0	0.3%
Henderson[22]	0.08$\rightarrow$ 0.18	0.313	NG	3×10^4	NG	0.14	NG
Zoccola[23]	0.02 0.04 0.08	0.18 $\rightarrow$ 0.73 0.09 $\rightarrow$ 0.36 0.055	NG	2.4×10^4	T	1.3	0.2%
Jacob et al,.[25]	0.3	11	1.14	6.8×10^6/m	T	0.027	NG
Jungowski et al.[26]	0.025 $\rightarrow$ 0.2	0.08 $\rightarrow$ 40	NG	0.1 $\rightarrow$ 16 $\times10^6$	T	NG	NG
Bruggeman et al.[27]	0.12, 0.22	NG	NG	High	NG	NG	NG
Bruggeman et al.[28]	0.0 $\rightarrow$ 0.044	$\sim$ 0.62	1.1	6.5×10^4	L	NG	NG
Ronneberger[31]	0.002	1	NG	6×10^3	L	$\sim$ 0.2	NG

Table 1 Parameter ranges for experiments with low Mach number flows.

Ref.	M	L/D	W/L	Re_L	δ/L	Turb. int.
Gates et al.[32]	0.6, 0.85, 0.95, 1.2	4.5, 9.0	0.22	1.04×10^8/ft	NG	
Plentovich[13]	0.3, 0.6, 0.85, 0.95	4.4, 11.7	0.23	3.5 $\rightarrow$ 14.7 $\times10^6$	0.014	NG
Tracy and Plentovich[16]	0.2, 0.6, 0.8, 0.9	4.4, 6.7, 12.67, 20.0	0.22	2 $\rightarrow$ 100 $\times10^6$	0.052 $\rightarrow$ 0.042	NG
Tracy and Plentovich[33]	0.6, 0.8, 0.9	4.4, 6.7, 12.67, 20.0	0.22	30 $\times10^6$	0.045	NG
Ahuja and Mendoza[6]	0.25 $\rightarrow$ 1.0	1.5, 2.5, 3.75, 6.0	<1 & >1	0.45$\rightarrow$ 1.2 $\times10^6$	$\sim$ 0.042	NG
Cattafesta et al.[34]	0.4, 0.6	2, 4	0.333	2.5 $\rightarrow$ 3 $\times10^6$	NG	NG
Shaw et al.[35]	0.7, 0.9, 1.2, 2.0	6.79, 10.27	NG	NG	NG	NG
McGrath and Shaw[36]	0.6, 0.8, 1.5, 1.9	2.56, 3.73, 6.83	>1	NG	0.13in/L	NG
Raman et al.[17]	0.6 $\rightarrow$ 1.32	3, 6, 8	0.43, 0.58, 1.17	2.4 $\times10^6$	NG	NG
Dix and Bauer[14]	0.95, 1.2, 5.04	4.5, 9.0, 14.4	0.22	4.5 $\times10^6$	NG	NG

Table 2 Parameter ranges for experiments with subsonic and transonic Mach number flows.

Ref.	M	L/D	Re_L	2D/3D	Exp. Comp	Method
Kriesels et al.[54]	low	1.0	high	2D	Same	Potential code
Hardin and Pope[1]	0.1	4.0	160,000	2D		IRANS + acoustics
Grace and Curtis[2]	0.1	8.0	10,000	2D		IRANS + acoustics
Curtis[58]	0.1	8.0	8,000	2D	[Ref.13], [Ref.78]	IRANS + acoustics
	0.26	4.0	20,000	2D	[Ref.13], [Ref.6]	
Kubotskii and Tam[38]	0.15	0.313	2.9×10^4	2D	[Ref.22]	RANS, DRP
Ashcroft et al.[39]	0.15	0.313	2.9×10^4	2D	[Ref.22]	RANS, $k-\omega$
Moon et al.[3]	0.15	0.313	2.9×10^4	2D	[Ref.22]	INS + acoustics
Shieh and Morris[61]	0.15	0.58	15,000	2D	[Ref.21]	RANS, DRP + SpAl + DES
Slimon[4]	0.26	0.5	160,000	2D		IRANS + $k-\epsilon$ + acoustics
Jacob et al.[25]	0.3	11	6.8×10^6	2D	Same	RANS+$k-\epsilon$ + LA
Shieh and Morris[5]	0.6	2.0	400,000	2D		
	0.4	4.4			[Ref.78], [Ref.13]	RANS. DRP + SpAl + DES
Shieh and Morris[40]	0.5	4.0	20,000	2D	"	"
Colonius et al.[53]	0.6	2.0, 4.0	5500	2D	[Ref.78]	DNS
Dougherty et al.[42]	0.6, 0.8, 1.2	20	1.65×10^6	2D	[Ref.78]	NS,TDV + BL
Fuglsang and Cain[43]	0.85	4.5	2.3×10^6	2D	[Ref.14]	RANS + BL + DNS
Srinivasan[63]	0.85	1.2	13.1×10^6	3D	SOFIA	RANS + BL
Venkatapathy et al.[47]	0.8	0.43	1×10^6	2D	SOFIA	RANS + BL
Srinivasan and Baysal[15]	0.58, 0.9	11.7, 4.4	1.6×10^6	3D	[Ref.13]	RANS + BLmod
Atwood[41]	1.2	NG	3.8×10^6	2D,3D		RANS + BL
Tu[76]	1.2	4.5	2.3×10^6	3D	[Ref.14]	MANS + 2BL
Suhs[50]	1.2	4.5	2.6×10^6	3D	[Ref.14]	DTNS + BL
Shih et al.[79]	1.5	5.0	1.09×10^6	2D	[Ref.80]	RANS + $\kappa-\epsilon$
Kim and Chokani[68]	1.5, 1.6	6,17.5	2×10^6	2D	See Same	RANS + CS
Zhang[48]	1.5, 2.5	3.0		2D	Same	MANS + $k-\omega$
Baysal and Stallings[72]	1.5	6,16,12	2×10^6	2D	Same	RANS + BL
Stanek et al.[77]	0.6, 1.2, 1.5	9.3		3D		RANS + $k-\epsilon$
Rizzetta[49]	1.5	5.0	1.09×10^6	3D	[Ref.80]	MANS + 2BL
Arunajatesan et al.[52]	1.47	6.0	7×10^6/ft	3D		LES/RANS + $\kappa-\kappa l$
Tam et al.[51, 75]	2.0	2.0	3.95×10^6	2D	Priv.	DTNS + MM
Sinha et al.[44]	2.0	4.5	3 [6]	3D	[Ref.14]	LES,RANS,+ MM
Gorski et al.[45]	2.36	6.2	6.66×10^6/m	3D	NG	NS,TVD, + BLmod
Baysal[46]		4.5		2D	[Ref.81]	RANS + BLmod
Baysal[74]	2.75	9	2.97×10^6	3D	[Ref.82]	RANS + BLmod

Table 3 Computational cavity simulations